

Diffraction-limited upgrade to ARGOS, the LBT's ground-layer adaptive optics system

Michael Hart, Lorenzo Busoni,¹ Oli Durney, Simone Esposito,¹ Wolfgang Gässler,² Victor Gasho, Sebastian Rabien,³ and Matt Rademacher

Center for Astronomical Adaptive Optics, The University of Arizona, Tucson, AZ 85721, USA

¹Osservatorio Astrofisico di Arcetri, Largo Enrico Fermi 5, I-50125 Firenze, Italy

²Max-Planck-Institut für Astronomie, Königstuhl 17, D-69117 Heidelberg, Germany

³Max-Planck-Institut für extraterrestrische Physik, Giessenbachstrasse, 85748 Garching, Germany

ABSTRACT

The Large Binocular Telescope (LBT) is now operating with the first of two permanently installed adaptive secondary mirrors, and the first of two complementary near-IR instruments called LUCIFER is operational as well. The ARGOS laser-guided ground-layer adaptive optics (GLAO) system, described elsewhere at this conference¹, will build on this foundation to deliver the highest resolution over the 4 arc min wide-field imaging and multi-object spectroscopic modes of LUCIFER. In this paper, we describe a planned upgrade to ARGOS which will supplement the Rayleigh-based GLAO system with sodium laser guide stars (LGS) to fulfill the telescope's diffraction-limited potential. In its narrow-field mode of 30 arc sec, LUCIFER will deliver imaging at the Nyquist limit of the individual 8.4 m apertures down to J band and long-slit spectroscopy with resolution up to 40,000. In addition, the LBT Interferometer² (LBTI) will cophase the two apertures, offering imaging at the diffraction limit of the 22.8 m baseline at wavelengths from 1.2 to 20 μm . In the first phase of the upgrade, a 10 W sodium LGS will be added to each half of the LBT, using the same launch telescopes mounted behind the two secondary mirrors as the Rayleigh LGS. The upgrade will rely on other components of the ARGOS infrastructure such as acquisition and guiding, and fast tip-tilt cameras. New wavefront sensors will be added to LUCIFER and LBTI. In the upgrade's second phase, the sodium and Rayleigh LGS will be used together in a hybrid tomographic sensing system. This configuration will offer the advantage that a single tip-tilt star will continue to be sufficient even for MCAO operation³, which is planned with LBT's LINC-NIRVANA instrument^{4,5}.

Keywords: Telescopes, adaptive optics, laser guide stars

1. LASER-GUIDED AO FOR THE LARGE BINOCULAR TELESCOPE

The Large Binocular Telescope (LBT), shown in Figure 1, is now the largest optical/infrared telescope in the world and for this and other reasons offers uniquely powerful scientific capabilities. In particular the 22.8 m baseline provided by the two primary mirrors, when cophased, will offer the highest spatial resolution for studies of faint objects, making the LBT arguably the forerunner of the next generation of Extremely Large Telescopes (ELTs). In common with other large telescopes around the world it will rely on adaptive optics (AO) to deliver high resolution imaging and spectroscopy. In fact the LBT was designed from the outset to include AO as an integral part of the telescope. Uniquely among telescopes of 8 m and above, the AO correction is built in to the LBT's adaptive secondary mirrors (ASM). This capability allows for correction of all instruments used at the Gregorian foci, without any requirement for relay optics that introduce losses and increase thermal background, complexity, and cost.

While first-light AO relies on natural guide stars (NGS), the LBT Observatory has launched a phased program to augment the telescope with laser-guided capability. Phase I, called the Advanced Rayleigh Ground layer adaptive Optics System



Figure 1. The Large Binocular Telescope on Mt. Graham, Arizona has two 8.4 m primary mirrors on a common mount.

(ARGOS) is now in advanced development. It will deploy six low-level Rayleigh LGS, three per aperture, to correct low-lying turbulence, which is isoplanatic over a wide field of view. This GLAO mode of operation will feed the 4 arc min wide-field modes of the LUCIFER near-infrared imagers and multi-object spectrographs with images that routinely reach $\sim 0.2\text{--}0.3$ arc sec resolution. The Phase I system passed a Final Design Review in March 2010, and is on track for deployment as a facility system in early 2012.

Phase II is to be developed concurrently. A sodium LGS will be added to each aperture using the same launch optics as the Rayleigh beacons. Additional wavefront sensors (WFS) will be deployed in front of the LUCIFERs with feedback to the ASMs. These instruments will then enjoy images sharpened to the diffraction limit of the individual 8.4 m apertures in the JHK wavebands.

Truly ground-breaking, however, will be the implementation of sodium LGS AO correction for the LBT Interferometer (LBTI). This instrument will bring together the beams from the two halves of the telescope in Fizeau mode, mimicking a filled pupil masked with two 8.4 m apertures. Imaging will be available with the full resolving power of the LBT with 22.8 m baseline at wavelengths from 2 to 20 μm , and with unique sensitivity in the thermal bands because of the minimal number of warm optics in the beam. High-quality AO control of the individual apertures will be provided by the sodium LGS and additional WFS placed in each arm of the LBTI, with piston control between the apertures provided by a K-band fringe tracker already built into the instrument. In addition, LBTI can be configured to operate as a Bracewell nulling interferometer, for which the laser AO will allow high-contrast investigation in the thermal IR of the environments of deeply embedded stars that are very faint in the optical.

In a further development, Phase III will combine use of the low-altitude Rayleigh and high-altitude sodium LGS into a uniquely powerful tomographic wavefront sensing system for multi-conjugate adaptive optics (MCAO). This hybrid sensing system will require just a single tip-tilt star for full multi-conjugate correction. Such a scheme overcomes a limitation of MCAO systems in which the beacons are all at a common range that leads to a requirement for three well separated tip-tilt stars^{3,6}. This is the case, for example, with the Gemini South MCAO system⁷ which will use five sodium LGS, but will be somewhat limited in its sky coverage by the need for multiple tip-tilt stars of magnitude ~ 18 or brighter within 1 arc min.

MCAO is already designed as an upgrade path into LBT's LINC-NIRVANA interferometer⁵, now nearing completion at the Max-Planck Institute for Astronomy in Heidelberg as a collaboration between LBT's German and Italian partners. Expected to be operational in 2011, LINC-NIRVANA will extend the full resolution of the coherently combined telescope apertures down to J band in the near IR with resolution as high as 10 milliarcsec. To give an example of its application, at this resolution, and with LBT's sensitivity, equivalent to a 12 m single aperture, stellar populations in galaxies at 5–20 Mpc will be resolved. For the first time, individual stars in giant elliptical galaxies will be within reach, allowing their star formation history to be investigated directly.

2. UPGRADE SYSTEM CONCEPT

The sodium laser AO system for the LBT is designed to satisfy a number of goals:

- Exploit the diffraction-limited imaging and spectroscopic modes of the LUCIFER instruments down to their shortest wavelengths.
- Expand the application of the coherent imaging and spectroscopic modes of the LBTI to faint and heavily reddened regions inaccessible to NGS AO.
- Provide a reliable, low maintenance system with low risk and minimal changes to existing telescope systems.
- Anticipate a further upgrade path to wide-field, modest Strehl, diffraction limited operation with MCAO.

The top level requirements for the system are listed in Table 1. We have chosen to implement them with sodium LGS. Early trade studies showed that while it may be possible under some conditions to approach the image quality requirements using tomographic analysis of the Rayleigh LGS already being implemented in the ARGOS ground-layer system, the Strehl ratio requirement will not generally be met with such low-altitude beacons. They are designed to be used at 12 km range, which only very poorly samples high altitude turbulence even at zenith. At lower elevation angles, the sampling becomes even worse, as does the strength of turbulence-induced aberration. A tomographic approach will therefore not be sufficient without a major re-working of the ARGOS design. In addition, the implementation of sodium LGS in Phase II of the LBT laser AO system moves us a huge step forward toward all-sky MCAO operation in Phase III.

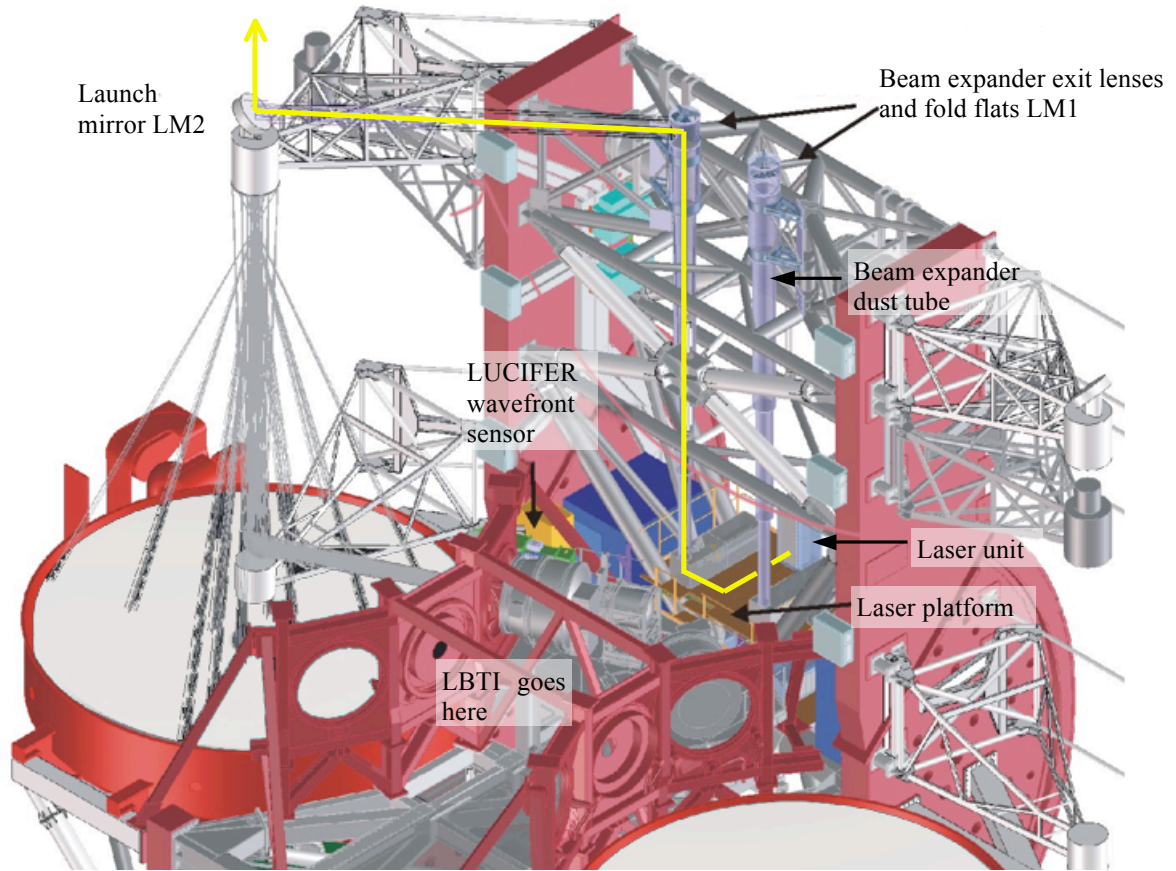


Figure 2. Layout on the LBT of the key components of the laser AO system. The facility can be divided roughly into the laser unit, the launch optics, the wavefront sensors, and the control system, which are further described in the text. The laser path for one side is shown in yellow.

Parameter	Requirement
Science wavelength regime	1.2–10 μm
Near IR image quality	K band Strehl ratio > 40% with bright on-axis tilt star under median seeing
Useable tip-tilt star	$V < 18$ up to 1' off axis
Useable seeing conditions	75 th percentile or better, r_0 (500 nm) > 13 cm
Elevation angle range	45° and above

Table 1. Top-level system requirements for the LBT's diffraction-limited laser AO system.

The system builds on existing infrastructure provided by LBT, and additional components under construction now for ARGOS. A schematic overview of the system as it will mount on the telescope is shown in Figure 2. The sodium system will take advantage of the ARGOS laser launch telescopes (LLT), which were specified in the Phase I design to accommodate both the Rayleigh laser wavelength of 532 nm and the sodium line at 589 nm. In addition, the sodium WFS in front of LUCIFER will be fed by the same dichroic beam splitter that separates the Rayleigh LGS light from the near IR science light. Other components will be shared as well: the ASMs, the real-time reconstructor computer, with appropriate extensions to its software, the laser safety interlock system which prevents the lasers from being propagated under any of a range of conditions, and the automatic aircraft detection system which guards against the illumination of aircraft by the beacon lasers.

2.1. Residual wavefront error and expected sodium return

The basic system design anticipates a guide star laser beam of 10 W above each eye of the LBT, with a final detected quantum efficiency at the WFS detectors of 40%. The WFS cameras will be identical for the LUCIFER and LBTI subsystems, and will put a 16×16 array of subapertures across each 8.4 m primary. Table 2 summarizes the wavefront error budget derived from these parameters. In calculating these values we have assumed the mean seeing at 500 nm for the LBT which is 0.65 arc sec. The atmospheric time constant τ_0 has been measured from DIMM data, and the median C_n^2 profile (from which the focal anisoplanatism is derived) has been measured in an extensive generalized SCIDAR campaign at the site⁹. Note that by design the largest term in the error budget for on-axis imaging is focal anisoplanatism: this is fundamental to a single-beacon AO system and so cannot be addressed by design improvements. Table 3 shows the corresponding anticipated Strehl ratios in the near IR bands both for tilt stars close to the science target and for the case where the star is 1 arc min off axis.

For calculations of the noise in the WFS, we assume conservatively that the photon return will be 3.4×10^5 photon/m²/s for 1 W of projected laser power, at a sodium column density of 1.5×10^9 cm⁻². This return is based on measurements by Ge et al.¹⁰ from the MMT using a narrow-band CW laser with circularly polarized output. The assumed column density is the seasonal minimum value found in measurements made at Kitt Peak, within a few hundred km and at the same latitude as the LBT site on Mt. Graham. For the *mean* measured density of 3.7×10^9 cm⁻² the sodium LGS will be just about a magnitude brighter.

Error budget term	WFE (nm)	Notes
<i>LGS high-order correction</i>		
Atmospheric fitting error	125	0.65" seeing ($r_0 = 16$ cm at 500 nm)
Telescope and instrument optics	74	M1—M3 = 34 each, dichroic = 20 instrument = 40
Time lag	48	$\tau_0 = 2.7$ ms at 500 nm, update rate = 500 Hz
WFS noise	73	Sandler et al. 1994 (assumes minimum sodium) ⁸
Focal anisoplanatism	142	From median C_n^2 profile, $d_0 = 4.2$ m at 500 nm
<i>NGS tip-tilt loop</i>		
Time lag	73	R=14 tip-tilt star assumed, loop running at 500 Hz
Sensor noise	67	
Anisokinetism (tip-tilt anisoplanatism)	291	Tilt star 60" off axis
<i>Other terms</i>		
Residual wind shake	102	Derived from MMT observations
Residual non-common path error	100	Budget allocation
Uncorrected Na layer focus	32	Experience at Keck II
TOTAL (on axis tilt star)	283	
TOTAL (tilt star 60" off axis)	406	

Table 2. Wavefront error budget for the sodium LGS AO system.

Waveband	J	H	K	L	M
On axis Strehl	0.27	0.41	0.57	0.78	0.88
Tilt star 60" off axis	0.14	0.23	0.37	0.62	0.77

Table 3. Predicted Strehl ratios from the AO system.

A 10 W sodium laser with circularly polarized output would give a minimum return of 1.4×10^6 photon/m²/s, assuming a detected quantum efficiency of 0.4, equivalent to a star of brightness $V=8.9$. This is about 1 magnitude brighter than the return seen at Keck II, which has output power about 10-14 W, during periods of minimum sodium density on Mauna Kea. The difference is attributable to the spectral format of the laser beam. It is confirmed by numerous measurements made at the Starfire Optical Range (SOR) using a single frequency circularly polarized CW beam¹¹. The SOR group in

fact finds a slightly better return even than the measurements of Ge et al.: the flux for 10 W of projected power, scaled to the same minimum sodium density, averages to 1.8×10^6 photon/m²/s, or typical guide star V magnitudes of 7-7.5 for average sodium densities.

2.2. Wavefront sensors

Two separate sets of wavefront sensor cameras will be required for the LUCIFERs and for LBTI. This is because the two instruments mount at two different bent-Gregorian foci on each half of the telescope, and they are selected by moving the tertiary mirrors which mount on rotating turrets. Laser beacon light, in common with science light, is reflected to the corresponding focus. In each case, however, cameras to acquire the sodium LGS on the WFS, and to provide the fast tip-tilt signal needed from starlight will already exist. Furthermore, because the WFS for both instruments must correct to high Strehl ratio in the K band, all four WFS cameras can be identical which achieves some economy of scale in their design and construction. In all cases, the sensors will have to ride on a longitudinal translation stage to accommodate the change in focus as the distance to the sodium layer changes with zenith angle.

The chosen design uses a 16×16 array of subapertures in a square geometry, each 0.525 m in size when projected onto the primary mirror. There are 204 subapertures with $>50\%$ illumination that will be used to recover the wavefront. As baseline, the WFS detectors will be the E2V CCD39, with an 80×80 pixel format of $24 \mu\text{m}$ pixels. We will adopt the successful approach used in the MMT WFS of bonding the lenslet array substrate directly to the chip carrier, as shown in Figure 3. This is feasible because by good fortune, the coefficients of thermal expansion of the substrate material, BK7, and the gray alumina of the chip carrier are almost identical. Each subaperture will cover a 4×4 pixel cell on the CCD, requiring a custom lenslet array with $96 \mu\text{m}$ pitch. We take a plate scale of 1 arc sec per pixel which implies a focal length for the lenslets of about 0.9 mm.

Ahead of each WFS will be a collimating lens of focal length 23 mm, designed to accept a beam at the telescope's native focal ratio of f/15. This will image the telescope's entrance pupil onto the lenslet array with the correct diameter of 1.53 mm. The opto-mechanical layout of the sensor head is shown in Figure 4. We require that the WFS focus be adjustable to allow for a range to the sodium layer of at least 85-140 km, these extremes accommodating a low mean sodium layer height at zenith, and a high mean height at 45° elevation. The required travel for the focusing stage is 74 mm. Our design adopts a stage with 100 mm of travel, requiring just $100 \mu\text{m}$ precision to avoid introducing focus errors in the science image. In addition, each head will be mounted on a motorized xy translation stage with a range of 10 mm and a precision of $10 \mu\text{m}$ to allow for remote alignment with the folded optical axis.

The anticipated frame rate of 500 Hz gives a flux of 770 photons per subaperture per exposure at the minimum sodium column density, with most of the signal concentrated in the central 4 pixels of each subaperture. A matched filter will be used to track the spot position, minimizing the effect of CCD read noise in the outer 12 pixels. The CCD39, read at 500 fps, has typically 4.5 electrons rms read noise. The effect of read noise will then be approximately equal to the photon noise of 27 electrons. The combined effect will be to contribute 73 nm rms to the residual wavefront error. During periods of increased sodium density, this residual error term will be correspondingly reduced.

The camera heads will be small thermoelectrically cooled dewars. They and the CCD controllers will be purchased from SciMeasure, matching the hardware already in hand for the NGS and ARGOS AO systems. The controllers have the flexibility to allow two readout modes: in one, the pixels will be binned 2×2 , effectively making quad cells of the subapertures. This has the advantage of reducing the readout time, and the latency in the AO servo loop, and the amount

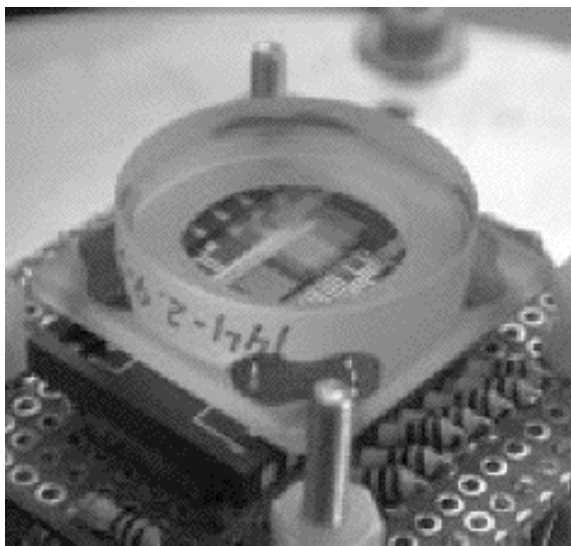


Figure 3. Photograph of the 6.5 m MMT's Shack-Hartmann WFS lenslet array, bonded to the CCD carrier with a BK7 shim.

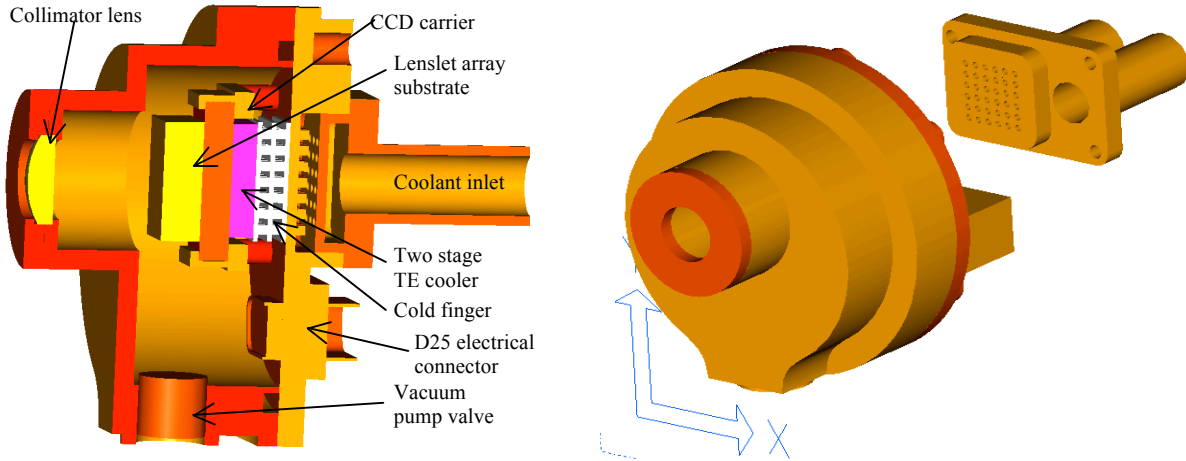


Figure 4. The CCD39 WFS head shown in section (*left*) and as a solid-body model (*right*) with the cooling plate removed. The diameter of the head at its widest is 75 mm.

of read noise included in the spot tracking calculation. In the second mode, the pixels will not be binned, and a correlation tracking algorithm will be used to find the spot centers. This mode has the advantage of finding a more accurate spot position.

Each of the four LGS WFS cameras will have a dedicated rack-mount control computer containing a single quad-core 3+ GHz CPU running Linux to handle the WFS camera readout and the corresponding slope calculations. These four LGS WFS control computers (LWCC) have only modest memory and disk space requirements and so can be purchased as commodity hardware. Each LWCC will require an EDT PCI-DV frame grabber card to interface with the camera controller and a single 10 GB ethernet interface card to connect to the real-time reconstructor computer.

These hardware requirements are scaled from current experience with the MMT's PC-based reconstructor computer used for the NGS AO system. It performs 210 slope calculations from 105 illuminated subapertures in approximately 60 μ s on a single 2.6 GHz CPU. Each LWCC on the LBT will perform 408 slope calculations in parallel on two CPUs. Thus, although the LBT must process twice as many slopes per aperture as the current MMT system, the LWCCs, each using 2 CPUs, will be able complete the slope calculations in well under 60 μ s. Since each WFS will have a dedicated LWCC, there will be no additional latency for camera readout operations compared to the existing MMT system that successfully operates at 560 Hz. The LWCCs will forward the slope measurements to the real-time reconstructor computer over the 10 GB ethernet interface. A dedicated 8-port 10 GB switch will isolate the network traffic consisting of LGS slopes.

2.2.1. Wavefront sensor system for LUCIFER

A large dichroic beam splitter in front of each LUCIFER separates the sodium beacon light from the infrared science light and reflects it toward the WFS. Note that since the WFS is fixed with respect to the telescope, and in particular with respect to the ASM actuator geometry, it does not need to rotate to counter the effect of the instrument rotator to which LUCIFER mounts.

The placement of the sodium WFS is shown in Figure 5. Following the beam splitter, a small elliptical fold mirror, 25 \times 40 mm, reflects the sodium LGS light down toward the LGS WFS. The mirror is positioned longitudinally so that it easily captures the footprint of the sodium beacon, which at that point varies between 10 and 15 mm diameter depending on the elevation angle, while avoiding vignetting the Rayleigh LGS beams. The clearance is 17 mm. With this arrangement, the mirror can stay in place permanently, and can be used in the Phase III system when the Rayleigh and sodium LGS are to be used together. The LGS WFS is positioned below the fold mirror, mounted on its triaxial translation stage.

Acquisition and fast guiding on the required tip-tilt star will be done with two cameras already installed in the LUCIFER acquisition, guiding, and wavefront sensing (AGW) units in support of the Phase I ARGOS system. This will rely on starlight between 0.6 and 1.0 μ m. In addition, the pyramid WFS in the AGW unit normally used for high-order NGS AO

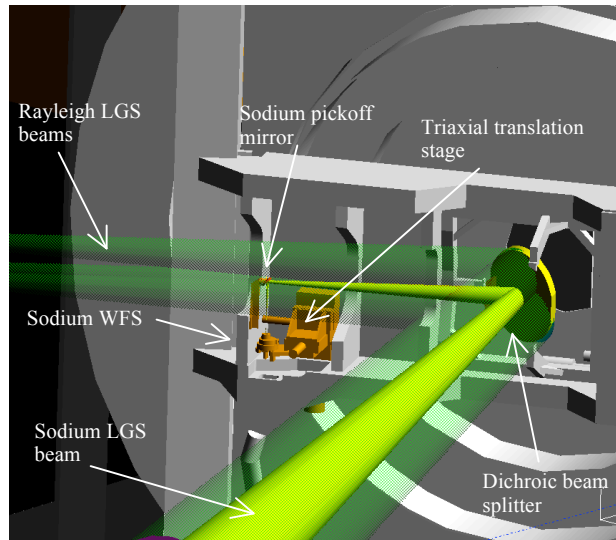


Figure 5. The ARGOS sodium WFS and dichroic beam splitter arrangement in front of LUCIFER. The Rayleigh LGS beams are also shown. The pickoff mirror for the sodium WFS fits in between the Rayleigh beams. The WFS, mounted on its triaxial translation stage, is shown in its fully forward position, corresponding to an elevation angle of 45° with the sodium layer at 140 km range.

will serve as the truth sensor. It will be run at slow speed, reading out roughly every 30 s, and will detect slowly varying wavefront aberration in the same way as the Keck II low-bandwidth WFS. The same approach has been very successfully adopted in the MMT's multi-LGS AO system. Focus measurements recorded by this sensor will be attributed to changes in the mean height of the sodium layer, and will be offloaded as DC offsets to the focus position of the LGS WFS camera. Experience at the Keck, the SOR, and other observatories is that such changes occur on timescales of a few minutes, much longer than the planned update rate from the NGS sensor.

2.2.2. Wavefront sensor system for LBTI

The entrance window to each arm of the LBTI cryostat is a dichroic beam splitter with similar characteristics to those of LUCIFER, though smaller because of the instrument's smaller field of view. Visible light from both the LGS and natural stars is reflected off them to the instrument's wavefront sensing ('W') units which are also near-copies of the LUCIFER AGW units. Each contains an E2V CCD47 acquisition camera with 14 arc sec FOV and a pyramid WFS which is normally used as a high-order sensor for NGS AO. The WFS puts up to 30×30 subapertures across the pupil, which can be reduced to 15×15 and 10×10 for increased sensitivity to faint stars simply by binning the CCD pixels by a factor of 2 and 3 respectively. Both cameras are mounted on a small optical breadboard which in turn mounts to a very stiff 3-axis translation stage with a patrol FOV of 3.6×2.2 arc min. A selectable beam splitter allows light from one star to be fed in a variable ratio to both the acquisition and pyramid WFS cameras. The z motion of the breadboard will allow the CCD47, normally used to acquire stars, to image the sodium beacon for acquisition as well.

For high-order wavefront sensing with the sodium LGS, a rugate filter, designed to reflect a 20 nm wide band centered on the sodium wavelength of 589 nm, is inserted after the LBTI entrance window. The filter rides on a translation stage so that it can be removed when not in use, to make way either for an artificial source used to calibrate the pyramid sensor, or to allow a clear path for reference starlight in NGS AO mode. The filter picks off the LGS light and sends it into the LGS WFS; it is nearly in the focal plane, and so can be small, about 10 mm in diameter, but must be of high quality to preserve the PSF seen by the WFS. The layout of the cameras and the optical path to the LGS WFS are shown in Figure 6.

When the LGS is in use, the acquisition and pyramid WFS cameras take on different roles. The natural star needed to sense global image motion will be put in one corner of the acquisition camera, next to the CCD's frame store mask. After transferring the accumulated charge into the storage area, only the first few rows of the 1024×1024 pixel device will be read out, with the rest dumped to prevent background charge from building up. The star image will be read out in this

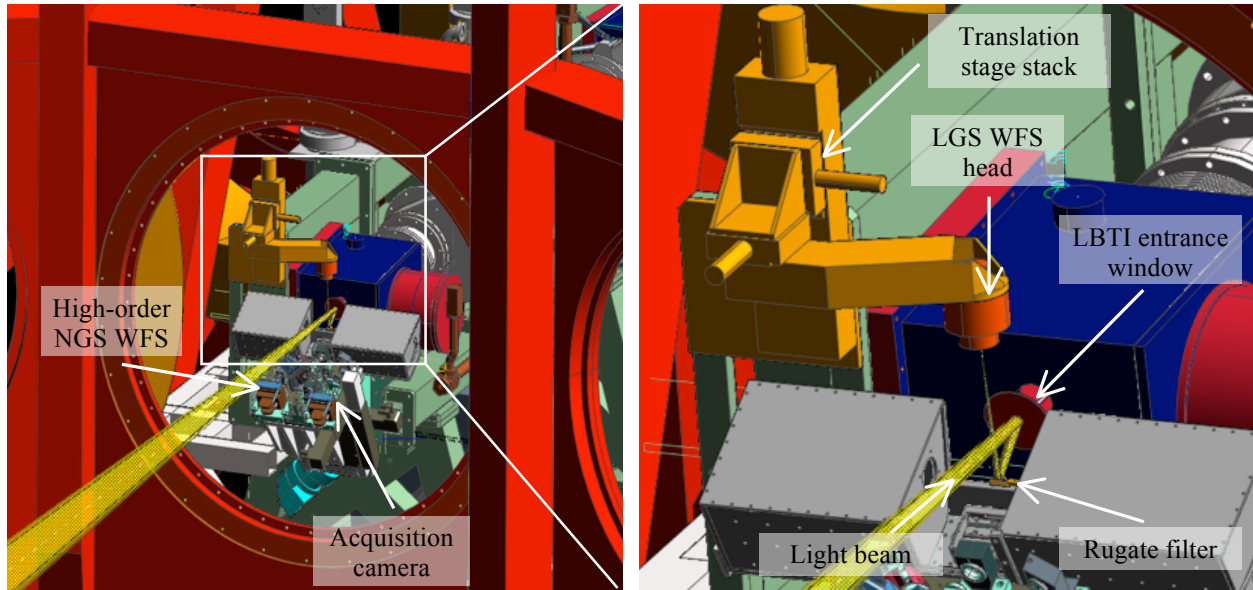


Figure 6. Placement of the LBTI sodium WFS. These pictures show a solid model of one arm of the instrument; the other is a mirror image. Incoming visible light reflects off the LBTI cryostat entrance window, tilted downward at 15° . A rugate filter placed near the infinity focal plane reflects the laser light up into the WFS, which is mounted on a 3-axis translation stage. The xy motion allows for alignment; the z motion accommodates changes in range to the sodium layer.

manner at frame rates up to 500 per second. The beam splitter dividing the starlight will be set to reflect a small fraction also into the pyramid WFS. This will be run as the truth sensor in the same way as described above for the LUCIFER channel.

Phase errors between the two halves of the telescope are sensed by a dedicated fringe tracking camera inside the LBTI cryostat. The camera has a small patrol radius of 5 arc sec, requiring an essentially on-axis phasing star with a K band magnitude of $K \leq 15$. Corrections are applied by two mirrors that can be moved in piston, one at low speed but with large stroke, the other a piezo-driven mirror that can respond quickly but has limited range. They are in corresponding locations in the optical train on opposite sides of the interferometer.

2.3. Control system

The laser AO control system will comprise a suite of software to carry out a range of automated procedures for alignment, implementing low-level control of the opto-mechanical assemblies, to read the WFS and acquisition cameras, synchronizing their data streams, and to supply real-time telemetry for system health monitoring and post facto analysis. The control system will be an extension of the software now under development for the ARGOS system and will use many of the same pieces, for example the real-time reconstructor machine and software, and the data archiving system.

2.3.1. Alignment

The alignment procedure to capture the LGS on the WFS camera and to acquire a tip-tilt guide star will be essentially identical for both LUCIFER and LBTI although the cameras used will not be the same. During system installation, the LGS will be bore-sighted with the telescope to within a few arc seconds, so it will be within the capture range of the acquisition cameras of both instruments. In all cases, the acquisition cameras are designed to operate with objects at infinity, not at the finite range of the LGS. In the case of LBTI, the focus motion of the stage carrying the camera will allow it bring the LGS into focus, but for LUCIFER, the telescope itself will have to be focused by moving the secondary mirror. Once the LGS is acquired, it will be steered using the launch telescope's LM1 mirror (shown in Figure 2) onto the projection of the LGS WFS axis on the acquisition camera. At that point, in the case of LUCIFER, the telescope will be refocused back to infinity.

Tip-tilt stars will be acquired for LUCIFER in the same way, and using the same software, as for the ARGOS system. For LBTI, the acquisition cameras will be run in full frame mode to identify the star, and the camera xy stages will be driven to place the star in one corner near the frame store mask. Then the cameras will be switched to the fast framing region-of-interest mode.

2.3.2. AO control architecture

To allow for modularity and ease of maintenance, the LGS AO controller is a decentralized system, that is, it will not rely on inputs from other LBT control systems such as active optics or pointing controls. To achieve the desired system performance, the LGS control architecture must minimize conflicting interactions with other existing LBT control components. Care must be taken to separate cross-talk between control elements in various spatial and temporal frequency regimes. In addition to supporting the AO modes directly, the controller must also be able to stabilize the outgoing laser beams against telescope vibrations and wind induced motions.

The LGS system must work in concert with several different LBT control components to perform effectively. Each control component operates over specific spatial and temporal frequency regions, illustrated in Figure 7. The primary frequency regimes are listed below.

- The low frequency regime consists of distortions to the primary mirror due to gravitational sag and thermal expansion. Active optics corrects these aberrations up to approximately 0.1 Hz. There is no significant interaction among control components in this regime.
- The Pointing Control System (PCS) is responsible for positioning the telescope line of sight. It has an effective bandwidth of approximately 3 Hz. The PCS can induce disturbances in the telescope which affect both the ASM and the fast tip-tilt mirror controlling the laser beam pointing in the LLT.
- AO is used to correct for high spatial and temporal frequencies. The ASM is used in all AO modes to correct for atmosphere turbulence effects.
- Cophasing of the two primary mirrors will be performed by the LBTI. Occasional offsets in piston will be offloaded to the secondary mirrors.
- LGS beam stabilization is accomplished in the LLT with a fast steering mirror at the full speed of the AO system.

Winds and other external disturbances can cause significant movement of the LGS beams with respect to the LBT's axis, which is seen as spot movement on the LGS wavefront sensor. While global tilt of the ASM is not controlled by the average LGS spot motion, large amplitude beam jitter can severely limit the dynamic range of the WFS and drive it out of the linear regime of its transfer function. Control of beam jitter with the fast steering mirror in the LLT driven by the average tilt measurement on the WFS is readily implemented, but experience at the MMT has shown that this may not adequately reduce the amplitude of the spot motion because of high frequency structural resonances. The problem has been very successfully addressed at the MMT through the use of accelerometers on the LLT there, running at 2 kHz read rate, with an empirical determination of the relationship between the accelerometer signals and global tilt on the WFS. The LBT will implement the same solution, using feedforward signals to minimize the effects of beam jitter. Figure 8 shows an overview of all the LBT control systems that will operate when LGS AO is running.

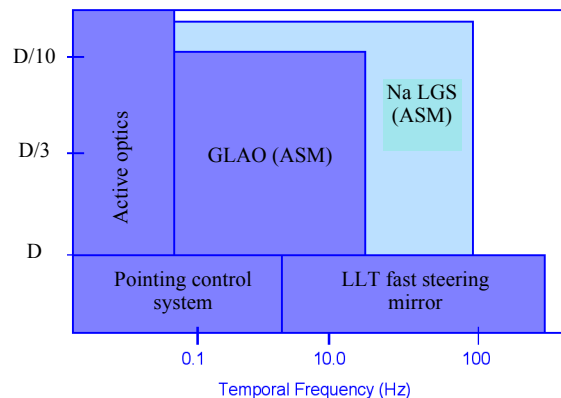


Figure 7. Spatial and temporal domains for LBT control components.

3. EXTENSION TO MCAO

The hybrid Rayleigh-sodium wavefront sensing scheme envisioned for the ARGOS upgrade offers greater potential than correction to the near IR diffraction limit over the conventional isoplanatic patch. It is a truly tomographic sensor,

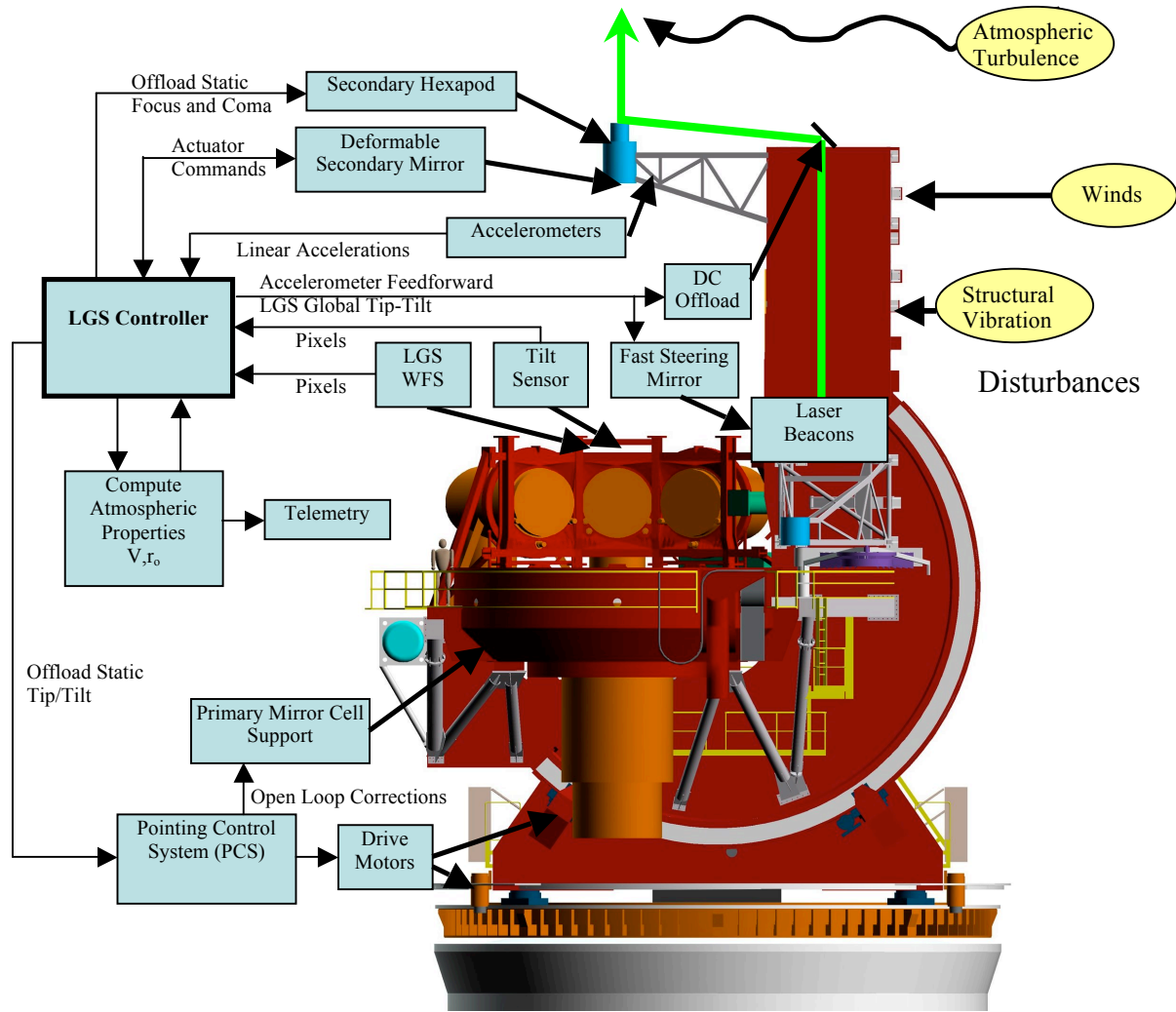


Figure 8. Overview of the control systems and disturbances that will be in effect during closed-loop operation of the sodium LGS AO system.

resolving the vertical distribution of the atmospheric turbulence. It is therefore well suited to driving a multi-conjugate corrector, where one or more additional deformable mirrors conjugated to high altitude supplement the ground-layer correction by the adaptive secondaries. Indeed, the arrangement described here has a crucial advantage for MCAO even when compared to systems such as the one being implemented on the Gemini South telescope. In that system, and the comparable Next Generation AO system under development for the Keck Observatory¹², all the laser beacons are at a common range from the telescope. The solution of the vertical distribution of focus and astigmatism is not possible in this case from the laser signals alone. In order to correct these modes over the full MCAO field, the single NGS needed by all laser systems to sense global image motion must be augmented by image motion measurements from two additional stars well separated in the field of view. The need for three NGS limits the area of sky that can be reached, particularly in dark fields of value for extragalactic work.

The mathematical degeneracy that prevents the solution of the second-order modes can also be broken by deploying LGS at two well-separated altitudes, as planned for ARGOS. In that case, the requirement for the NGS is reduced again to the measurement of image motion from a single star and the full sky coverage expected from a LGS system is restored. In this way, we expect to extend the application of ARGOS to LINC-NIRVANA, LBT's interferometric instrument that includes provision for a second high-altitude deformable mirror in each arm, to give diffraction-limited near IR resolution over its full field. In addition, a third generation of spectroscopic instruments would be enabled employing multi-object AO with MEMS deformable mirrors to cover fields up to 2 arc min in diameter.

4. CONCLUDING REMARKS

The three-phase implementation of laser-guided AO at the LBT employs innovative techniques to exploit the unique features of the LBT. The telescope's adaptive secondary mirrors, conjugated to the boundary layer of turbulence, are ideal for wide-field ground layer correction which ARGOS will realize in Phase I with low-cost low-altitude Rayleigh LGS. The secondaries also afford high sensitivity in the thermal IR which will be exploited with the sodium laser in Phase II by the cameras of the LBT Interferometer, now at the diffraction limit of the combined aperture with the resolution of a 22.8 m baseline. Finally, in Phase III, with the Rayleigh and sodium lasers operating as a unified hybrid sensing system, wide-field imaging at the combined-aperture diffraction limit will be enabled with MCAO.

5. REFERENCES

- [1] Rabien, S. et al., "ARGOS: the laser guide star system for the LBT," these proceedings.
- [2] Hinz, P. M. et al., "The Large Binocular Telescope Interferometer," in *Interferometry for Optical Astronomy II*, ed. W. A. Traub, Proc. SPIE **4838**, 108 (2003).
- [3] Lloyd-Hart, M. and Milton, N. M., "Fundamental limits on isoplanatic correction with multiconjugate adaptive optics," JOSA A **20**, 10, 1949 (2003).
- [4] Egner, S. E. et al., "LINC-NIRVANA: the single arm MCAO experiment," in *Advances in Adaptive Optics*, eds. D. Bonaccini, B. L. Ellerbroek, and R. Ragazzoni, Proc. SPIE **5490**, 924 (2004).
- [5] Egner, S. E. "Multi-Conjugate Adaptive Optics for LINC-NIRVANA: Laboratory tests of a Ground-Layer Adaptive Optics System and Vertical Turbulence Measurements at Mt. Graham," Ph.D. dissertation, University of Heidelberg, (2006).
- [6] De La Rue, I. and Ellerbroek, B. L., "Multiconjugate adaptive optics with hybrid laser beacon systems," in *Adaptive Optics Systems and Technology II*, eds. R. K. Tyson, D. Bonaccini, and M. C. Roggemann, Proc. SPIE **4494**, 290 (2002).
- [7] Bec, M. et al., "The Gemini MCAO bench: system overview and lab integration," in *Adaptive Optics Systems*, eds. N. Hubin, C. E. Max, & P. L. Wizinowich, Proc. SPIE **7015**, 701568 (2008).
- [8] Sandler, D. G., Stahl, S., Angel, J. R. P., Lloyd-Hart, M., and McCarthy, D. W., "Adaptive Optics for Diffraction-Limited Infrared Imaging with 8 m Telescopes," JOSA A **11**, 925 (1994).
- [9] Egner, S. E. et al., "Generalized SCIDAR Measurements at Mount Graham," PASP **119**, 669 (2007).
- [10] Ge, J. et al., "Mesosphere Sodium Column Density and Laser Guide Star Brightness," Proc. ESO workshop on Laser Technology for Laser Guide Star Adaptive Optics, 10-15, Garching, (1997).
- [11] Denman, C. A. et al., "Characteristics of sodium guidestars created by the 50-watt FASOR and first closed-loop AO results at the Starfire Optical Range," Proc. SPIE **6272**, 62721L (2006).
- [12] Wizinowich, P. L. et al., "W. M. Keck Observatory's next-generation adaptive optics facility," Proc. SPIE **7015**, 701511 (2008).